Organic & Biomolecular Chemistry

Cite this: *Org. Biomol. Chem.*, 2011, **9**, 5137

www.rsc.org/obc

PAPER

Pyrroloquinoxaline hydrazones as fluorescent probes for amyloid fibrils†

Sandra Gemma,[a,b] Laura Colombo,[a,c] Gianluigi Forloni,[a,c] Luisa Savini,[a,b] Claudia Fracasso,[a,c] Silvio Caccia,[a,c] Mario Salmona,[a,c] Margherita Brindisi,[a,b] Bhupendra P. Joshi,[a,b] Pierangela Tripaldi,[a,b] Gianluca Giorgi,[d] Orazio Taglialatela-Scafati,[a,e] Ettore Novellino,[a,f] Isabella Fiorini,[a,b] Giuseppe Campiani*[a,b] and Stefania Butini[a,b]

Received 22nd February 2011, Accepted 14th April 2011
DOI: 10.1039/c1ob05288h

Here we describe the identification and preliminary characterization of a new class of pyrrolo(imidazo)quinoxaline hydrazones as flurescent probes for $A\beta_{1-42}$ fibrils. All the newly developed compounds were able to bind amyloid fibrils formed *in vitro* and some of them displayed an increase of their fluorescence upon binding. When tested on brain tissue preparations presenting Aβ deposits, the described hydrazones selectively stained amyloid structures and did not display aspecific binding. The hydrazones did not show antifibrillogenic activity and electron microscopy analysis revealed that they do not interfere with fibrils structure. The described pyrrolo(imidazo)quinoxalines could be useful for studying amyloid structures *in vitro*. Moreover, their experimentally proven ability to cross the blood–brain barrier in mouse opens the possibility of developing these compounds as potential amyloid imaging agents for *in vivo* applications.

Introduction

A fluorescent probe is a molecular system able to produce a detectable fluorescent signal upon interaction with a chemical species. An extremely important field of application of fluorescent probes is the detection of amyloid fibrils, highly organized fibrillar aggregates characterized by a β-pleated sheet structure. Amyloid fibrils are a fundamental feature of several disorders collectively designated as protein misfolding disorders. Among them, Alzheimer's disease (AD) is characterized by the formation of amyloid plaques, which are composed by fibrils of 40–42 amino acid peptides termed β-amyloid (Aβ). The detection of amyloid deposits in affected brain tissues, as well as the evaluation of fibrillogenesis and fibrillation kinetics *in vitro* are important areas of intense research.[1–3] Two fluorescent probes such as thioflavin T (ThT, **1**, Fig. 1) and Congo Red (**2**), have been widely used for studying amyloid fibrils. These compounds characteristically stain amyloid-like deposits and specifically interact with the crossed-β-sheet structure of amyloid. ThT and similar fluorogenic

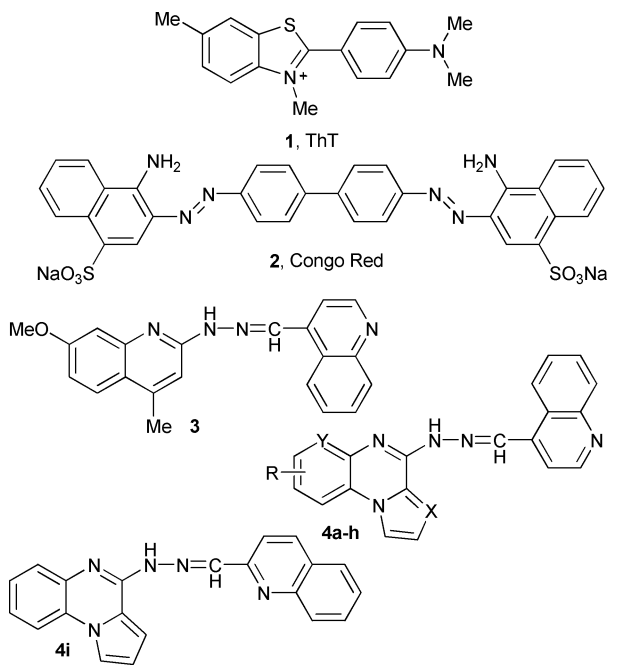

Fig. 1 Reference and title compounds. R, X and Y are defined in Scheme 1.

[a]*European Research Centre for Drug Discovery and Development (NatSynDrugs), University of Siena, via Aldo Moro, 53100, Siena, Italy. E-mail: campiani@unisi.it; Fax: 39 0577 234333; Tel: 39 0577 234172*
[b]*Dip. Farmaco Chimico Tecnologica, University of Siena, via Aldo Moro, 53100, Siena, Italy. E-mail: campiani@unisi.it; Fax: 39 0577 234333; Tel: 39 0577 234172*
[c]*Istituto di Ricerche Farmacologiche "Mario Negri" (IRFMN), Via la Masa 19, 20156, Milano, Italy*
[d]*Dip. di Chimica, University of Siena, via Aldo Moro, 53100, Siena, Italy*
[e]*Dip. di Chimica delle Sostanze Naturali, Università di Napoli Federico II, via D. Montesano 49, 80131, Napoli, Italy*
[f]*Dip. di Chimica Farmaceutica e Tossicologica, Università di Napoli Federico II, via D. Montesano 49, 80131, Napoli, Italy*
† CCDC reference numbers 612697, 612698. For crystallographic data in CIF or other electronic format see DOI: 10.1039/c1ob05288h

compounds are broadly used for detecting cellular components and structures *in vitro* but are not able to cross the blood–brain barrier (BBB). On the other hand several uncharged agents with the backbone structure of ThT and Congo Red have been synthesized and evaluated for *in vivo* use as probes to image amyloid plaques in AD brain.[4–14]

We have been recently interested in the field of amyloid binding agents and in particular in developing fluorescent probes for amyloid fibrils to be used for *in vitro* histochemical and cellular characterization of amyloid structures. We recently proved that specific 2-quinolylhydrazones typified by **3** (Fig. 1) were able to bind amyloid fibrils *in vitro* and, after oral administration, stained amyloid deposits in the brain of transgenic mice carrying the human gene for β-APP.[15] Moreover, detection of amyloid plaques in mouse brain preparations was readily accomplished by the distribution of compound-associated fluorescence. Although the binding mode has not been defined at atomic level yet, linear dyes such as ThT are believed to bind to extended channel-like motifs along solvent-exposed surfaces of fibrils, in turn formed by side chains of amino acids of the β-sheet structures. A striking feature of ThT is the fluorescence enhancement which is observed upon binding to fibrils.[16,17] This feature has been intensively studied suggesting that the fluorescence behaviour of ThT is related to the rotation of the aniline and benzothiazolium rings around their shared carbon-carbon bond. Although Dzwolak and co-workers hypothesized that ThT is significantly twisted when bound to amyloid,[18] most studies suggest that ThT binding to amyloid fibrils probably immobilizes the ThT aniline and benzothiazolium rings in a flat conformation, resulting in a high quantum yield of fluorescence.[19] The uncharged compound **3**, formed by two aromatic systems conjugated through a hydrazone linker, is likely to have a binding mode to amyloid fibrils similar to that of ThT.

With the aim of improving the binding affinity of **3** for amyloid fibrils, we decided to replace the 4-methylquinolyl system of **3** with a pyrroloquinoxaline moiety (compound **4a**, Fig. 1) in order to increase the contact surface of the resulting compound within the channel. During this study we discovered that introduction of the pyrroloquinoxaline system strongly favored an almost flat conformation of the whole system due to extensive conjugation of the two heteroaromatic moieties through the hydrazone linker. Starting from **4a**, a small set of analogues was synthesized in order to preliminarly evaluate the effect of differently substituted policyclic scaffolds for Aβ binding. In particular, different substituents at the benzofused ring (**4a–e**) were introduced, the benzo-fused ring of **4a** was replaced by a pyridine (**4f**), the pyrrole-fused ring by an imidazole (**4g**,**h**) and the 4-quinoline by a 2-isoquinoline moiety (**4i**). Here we report the synthesis, structural analysis, amyloid binding properties, and fluorescent characterization in the presence of amyloid fibrils of compounds **3** and **4a–i** (Scheme 1).

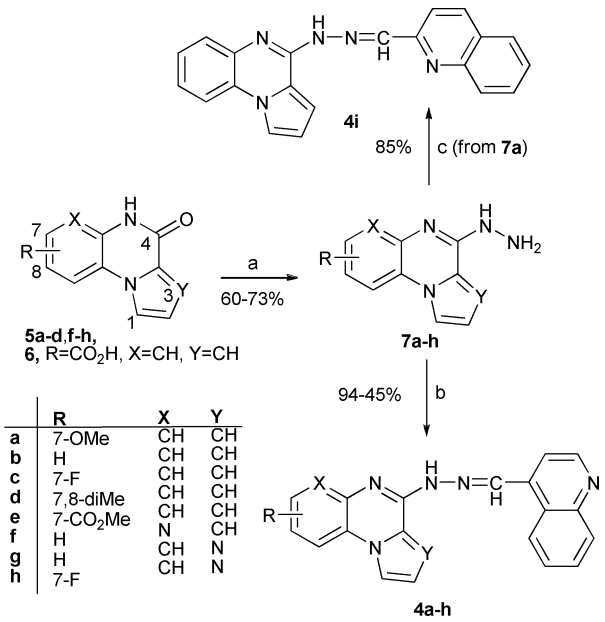

	R	X	Y
a	7-OMe	CH	CH
b	H	CH	CH
c	7-F	CH	CH
d	7,8-diMe	CH	CH
e	7-CO_2Me	N	CH
f	H	CH	N
g	H	CH	N
h	7-F		

Scheme 1 Synthesis of hydrazones **4a–i**. a) i. $POCl_3$, *N*,*N*-dimethylaniline, 120 °C, 2–4 h (from **6**: $POCl_3$, *N*,*N*-dimethylaniline, 120 °C, 4 h, then methanol, 25 °C, 5 min); ii. $NH_2NH_2 \cdot H_2O$, ethanol, 90 °C, 2–4 h; b) quinolin-4-carboxaldehyde, ethanol, 90 °C, 4 h; c) quinolin-2-carboxaldehyde, ethanol, 90 °C, 6 h.

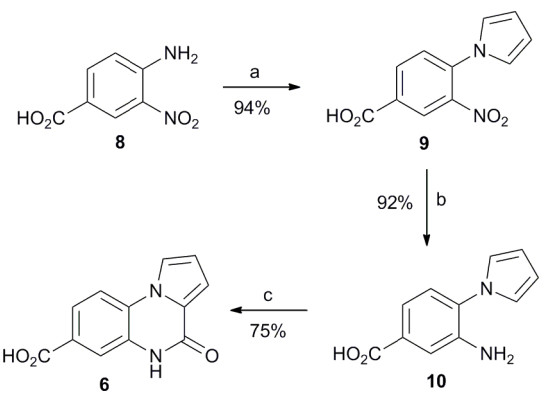

Scheme 2 Synthesis of lactam **6**. a) Dimethoxytetrahydrofuran, AcOH, 120 °C, 1 h; b) Pd/C, H_2 (1 atm), 1 : 1 EtOAc/MeOH, 14 h; c) triphosgene, toluene, reflux, 4 h.

Results and discussion

Chemistry

The synthesis of the target compound **4a–i** was performed as depicted in Schemes 1 and 2. Lactams **5a–d**,**f–h**[20] and **6** (Scheme 1) were converted into the corresponding chlorides by treatment with phosphorous oxychloride in the presence of *N*,*N*-dimethylaniline and these latter compounds were reacted with hydrazine monohydrate in refluxing ethanol to afford hydrazino-derivatives **7a–h**. In the last step of the synthesis, a mixture of hydrazines **7a–h** and quinolin-4-carboxaldehyde or quinolin-2-carboxyaldheyde in ethanol was heated under reflux to furnish the desired hydrazones **4a–i** in good overall yield. The final compounds were purified by means of flash-chromatography followed by crystallization from ethanol.

Lactam **6**, necessary for the synthesis of hydrazone **4e** was prepared starting from the carboxylic acid **8** (Scheme 2) that was converted into the corresponding pyrrole **9** applying the Clauson–Kaas protocol. The nitro-group of **9** was reduced by catalytic hydrogenation in the presence of palladium on carbon as the catalyst and the aniline **10** thus obtained was finally cyclized to lactam **6** by treatment with triphosgene in toluene.

Structural analysis

NMR investigation of the target compounds revealed that their proton spectra, performed in DMSO-d_6 presented two different sets of signals in almost 1 : 1 ratio. To investigate the structures of these hydrazones, we decided to analyze a representative compound both in solid phase (through X-ray diffraction) and in solution (through NMR techniques). Depending upon the crystallization solvent, compound **4a** crystallized in two polymorphic structures (**4a**$_a$ from EtOH and **4a**$_b$, from MeOH). Both structures (Fig. 2A,B) showed a single bond between the two pendant nitrogen atoms and a double bond between N15 and the quinoxaline ring (tautomer A, Fig. 3). This caused the formation of an intramolecular hydrogen bond N(1)–H···N(16) with H···N distances of 2.36 and 2.24 Å for **4a**$_a$ and **4a**$_b$, respectively. The two polymorphic structures showed quite similar geometrical and conformational parameters with the exception of the orientation of the methoxy group. The dihedral angles formed by the pyrroloquinoxaline and the quinoline rings are 10.58(1)° and 12.65(11)° for **4a**$_a$ and **4a**$_b$, respectively.

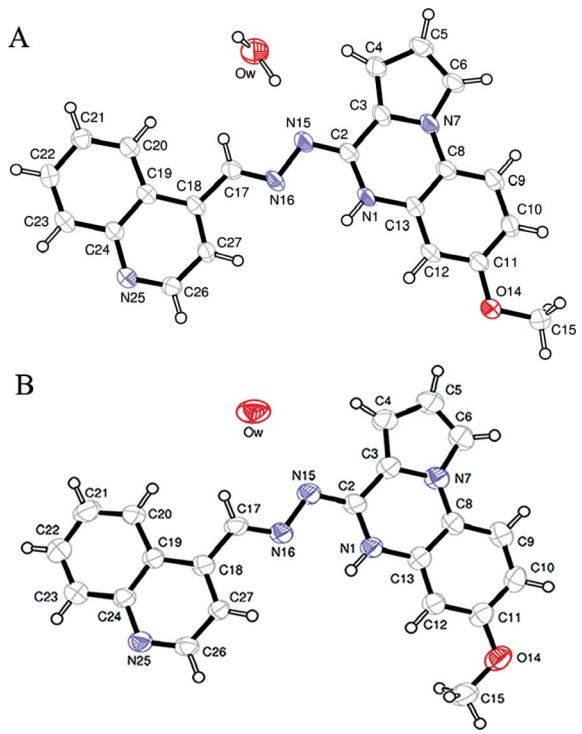

Fig. 2 X-ray crystal structures of **4a** in the two polymorphic forms. A. Crystallization from EtOH (**4a**$_a$); B. Crystallization from MeOH (**4a**$_b$) with the disordered methanol omitted for clarity.

Although it is described that heterocyclic hydrazones can present different prototropic tautomeric equilibria involving their acidic hydrogen,[21,22] stable imino-derivatives of heterocyclic hydrazones are not common features of these class of compounds and only a few examples have been previously reported in the literature including a neutral phthalazinylhydrazone reported by us,[23] and the imino tautomers of 2-quinolylhydrazone derivatives.[24,25]

Taking into consideration the above results and the observation that the NMR signal splitting was particularly evident only for protons of the quinoxaline ring, we hypothesized that the two set

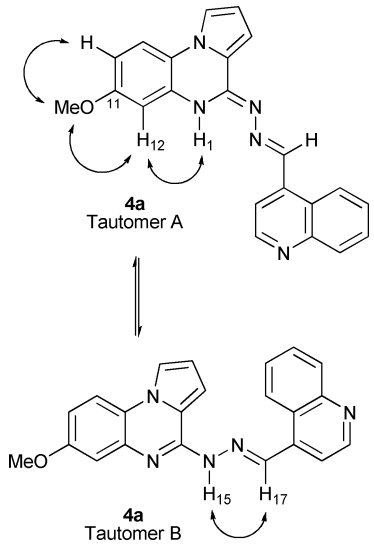

Fig. 3 Prototropic tautomers A and B exemplified for compound **4a**. Observed NOE effects are indicated by double arrows. Numbering from Fig. 2.

of signals observed in the NMR spectra of all compounds could be due to the co-existence in solution of the two equilibrating tautomers A and B (indicated in Fig. 3 for compound **4a**). To test this hypothesis, we first assigned the two series of ^{1}H NMR signals in DMSO-d_6 for the mixture of tautomers of **4a** through interpretation of 2D NMR spectra (COSY, HSQC, HMBC). Two different exchangeable protons were evident in the ^{1}H NMR spectrum at δ_H 10.70 and 11.80, respectively, assignable to the N-linked protons present in tautomers A and B. Cross-peaks exhibited by these key signals in the 2D NMR ROESY spectrum (see Fig. 3) were then utilized to obtain their unambiguous structural localization, thus also supporting the structures proposed for the two different tautomers. In particular, the signal at δ_H 10.70 showed ROESY cross-peak with H-12 (in turn spatially coupled to the methoxy group at C-11) and was therefore assigned to NH-1, in agreement with the structure of tautomer A. On the other hand, the exchangeable signal at δ_H 11.80 showed ROESY cross-peak with the imine proton at δ_H 9.32 (H-17) and was therefore assigned to NH-15, in agreement with the structure of tautomer B.

The existence of tautomers A and B was also observed by RP-HPLC analysis revealing the presence of two peaks for each compound after isocratic elution with methanol or acetonitrile. Isolation of the two peaks was not possible due to rapid equilibration in solution.

Differently from compounds **4a–i**, the quinoline derivative **3** did not show tautomeric equilibrium, as indicated by the single peak displayed during HPLC analysis and by the single set of signals in the proton NMR spectrum recorded in DMSO-d_6. It can be argued that the presence of the pyrrole ring in structures **4a–i** has the effect of weakening the aromatic stability of the condensed six-membered ring, thus rendering energetically feasible the existence of the tautomer with exocyclic double bond.

Table 1 Calculated logP for compounds **4a–i** and **3**, effect of treatment of pre-formed fibers of $A\beta_{1-42}$ with compounds **3**, **4a–i** on the fluorescence signal of ThT and quantification of their anti-aggregation properties

Compd	CLogP[a] TA	TB	UAF (Ex = 420 – Em = 480)[b]	Reduction of ThT fluorescent signal (%)	Reduction of preformed Aβ fibrils (%)[c]
ThT, **1**	—	—	356.0 ± 11.5	—	—
4a	6.2	4.3	103.3 ± 8.5	71	—
4b	5.8	4.1	49.4 ± 6.1	86	—
4c	5.5	4.3	74.9 ± 8.1	79	0
4d	6.7	4.5	159.2 ± 8.3	55	34
4e	6.4	4.5	347.3 ± 5.9	2	—
4f	4.7	4.4	198.0 ± 10.9	44	6
4g	5.2	4.4	203.2 ± 16.8	43	10
4h	5.0	4.5	154.1 ± 13.5	57	11
4i	6.4	4.7	181.1 ± 3.6	40	—
3	6.5	—	143.9 ± 16.4	60	—

[a] ACD/logP, version 11.00, Advanced Chemistry Development, Inc., Toronto, Canada). [b] ThT Fluorescence signal intensity measured at the excitation and emission wave lengths of 420 and 480 nm, respectively after incubation with the tested compound for 5 min. The fluorescence values of the samples containing only tested compounds was determined and subtracted from the values of the samples containing $A\beta_{42}$ fibrils and compounds. [c] Quantification of the amount of aggregated Aβ peptide after exposure to the tested compounds was performed by HPLC.

Interference with ThT binding and electron-microscopy analysis

Compounds **4a–i** were tested for their ability to interfere with ThT staining of pre-formed $A\beta_{1-42}$ fibrils. Therefore, the compounds at a concentration of 10 μM were incubated for 30 min in the presence of $A\beta_{1-42}$ fibrils before the ThT binding was measured. As illustrated in Table 1, all compounds, with the exception of **4e**, were able to interfere with ThT fluorescence. The extent of the fluorescent signal reduction ranged from a maximum of 87% for **4a** to a minimum of 40% for **4i**.

Electron microscopy (EM) analysis performed on fibers exposed to compounds **3** and **4a**,**b** allowed a direct examination of self-assembling capacity of the peptide. EM microphotographs (Fig. 4) showed structured amyloid fibrils obtained with $A\beta_{1-42}$ after an incubation period of 5 days (Panel A). The presence of compounds **3**, **4a**,**b** (Panels B–D) during the incubation time induced some changes but substantially did not alter the structure of the fibrils. Thus, the observed reduction of fluorescent signal of ThT is likely due to displacement of the staining by compounds **3**, **4a**,**b** and cannot be ascribed to an anti-fibrillogenic capacity of pyrroloquinoxaline hydrazones **4a**,**b** and quinolylhydrazone **3**. The observation that binding to the fibers was not associated with anti-aggregation capacity of the examined compounds was further investigated for **4c**,**d**,**f**,**g** by the direct quantitative determination of $A\beta_{1-42}$ peptide by HPLC in the pellet after five days of incubation and the centrifugation of the peptide solution. The co-incubation of $A\beta_{1-42}$ (in the proportion 1 : 1) with the different compounds did not significantly reduce the amount of the peptide found in the pellet with respect to the control (Table 1).

Fluorescence measurements

The fluorescence behaviour of the compounds in the presence and in the absence of amyloid fibrils was also analyzed. The spectrum of **3** was accurately analyzed (Fig. 5) at different incubation times (Fig. 5C) or concentrations (Fig. 5D) with or without fibrils. The incubation time did not substantially affect the results while the spectra alteration progressively increased with the compound concentration. After standardization of the experimental conditions for compound **3**, the other compounds were tested at a single time and at the higher concentration of 10 μM. All compounds presented a certain level of fluorescence that is strongly (Fig. 6) or modestly altered (Fig. 7) when mixed with $A\beta_{1-42}$ fibrils similarly to ThT (Fig. 5A).

Staining of amyloid deposits in CRND8 Tg mice

The ability of compounds **3**, **4a**,**b** and **4f**,**g** to bind amyloidogenic structures was tested in brain sections from CRND8 transgenic mice. These animals carry human APP with double mutations and accumulate Aβ deposits in brain parenkyma and at cerebrovascular level.[26] Five-micrometre-thick serial sections of paraffin-embedded blocks from frontal cortex were used for staining. Tissue sections were covered with a solution of EtOH 96% with the different compounds at the concentration of 0.5 mM. Fluorescent sections were viewed using fluoromicroscope equipped with filters UV, FITC and TRITC. The binding of fluorescent compounds to amyloid deposits was compared to the staining obtained with Congo Red and thioflavin S (ThS), that specifically bind amyloid structures in adjacent sections. With the exception of **3**, for all the other compounds (**4a**,**b**,**f**,**g**) the intensity of the fluorescent signals was similar to those obtained with Congo red or ThS either in the parenchyma (Fig. 8) or on the vascular walls (Fig. 9). These results suggested that the newly developed compounds recognize the β-pleated sheet structure of amyloid fibrils similarly to standard dyes, like ThS or Congo Red and that they are not involved in aspecific binding to tissue preparations.

Brain-to-plasma distribution studies

Crossing of the BBB is a key aspect to develop potential tools for diagnosis. Brain permeability studies were carried out to evaluate the potential application of these non-charged amyloid probes as imaging agents in PET techniques. Hydrazones examined in this study were characterized by high calculated logP values as indicated in Table 1, predictive of their ability to cross the BBB. In order to experimentally prove the brain permeability of this

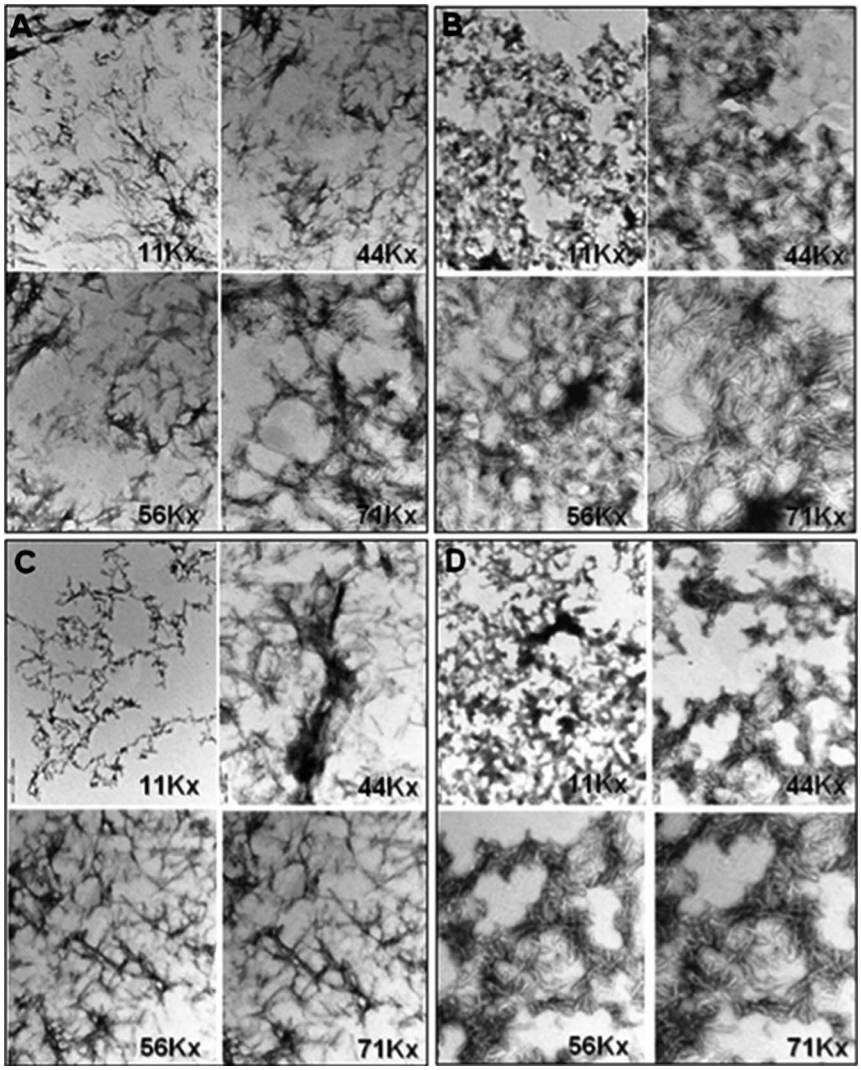

Fig. 4 Electron microscope microphotographs structured amyloid fibrils obtained with $A\beta_{1\text{-}42}$ (Panel A) and after co-incubation with **3** (Panel B), **4a** (Panel C), and **4b** (Panel D).

class of amyloid fluorescent probes, a preliminary evaluation of the distribution between plasma and brain of compound **4c** was performed in an animal model. The doses of compound **4c** (1.25–10 mg kg^{-1}, dissolved in PEG-400 : DMSO : ethanol) and route of administration (intraperitoneal) were derived from previous studies with structurally related derivatives.[27] In plasma, compound **4c** reached the highest mean concentrations at 30 min; these concentrations appeared to be dose proportional between 1.25 (173 ± 13 ng mL^{-1}) and 2.5 mg kg^{-1} (506 ± 39 ng mL^{-1}) but slightly less than proportional at higher doses (540 ± 303 and 737 ± 211 ng mL^{-1}, at 5 and 10 mg kg^{-1}, respectively), possibly reflecting dose related variability in the rate or extent of absorption from the injection site. At the lower doses these plasma concentrations were low and variable and rapidly fell below the limit of quantitation after 2 h (<125 ng mL^{-1}, using 0.2 mL of mouse plasma). At the 10 mg kg^{-1} dose, mean plasma concentrations at 2 h were less than one-third those at 30 min (720 ng mL^{-1} or about 2 μM), and at 8 h they were below the limit of quantitation of the analytical procedure (125 ng mL^{-1}, using 0.2 mL of mouse plasma).

In brain, the compound concentrations were about three times higher than plasma concentrations regardless of the dose and sampling time (435 ± 59, 1211 ± 214, 1413 ± 663 and 1522 ± 477, at 1.25, 2.5, 5 and 10 mg kg^{-1}). As shown in Fig. 10 there was a linear relationship between plasma and brain concentrations 30 min after dosing (brain = 233 + 1.96 plasma; $r^2 = 0.85$). This linear relationship further suggests that compound **4c** crosses the BBB by passive diffusion, with plasma concentrations consistently reflecting the whole brain concentrations. These preliminary data make this class of compounds promising lead structures for further development as amyloid imaging agents to be used as diagnostic tools. Their prospective development as diagnostic imaging agents is further justified by the promising results obtained with the fluorine analogue **4c** that could be labelled for PET application.

Conclusions

A new series of pyrroloquinoxaline hydrazones characterized by affinity for both $A\beta_{1\text{-}42}$ fibrils aggregated *in vitro* and Aβ

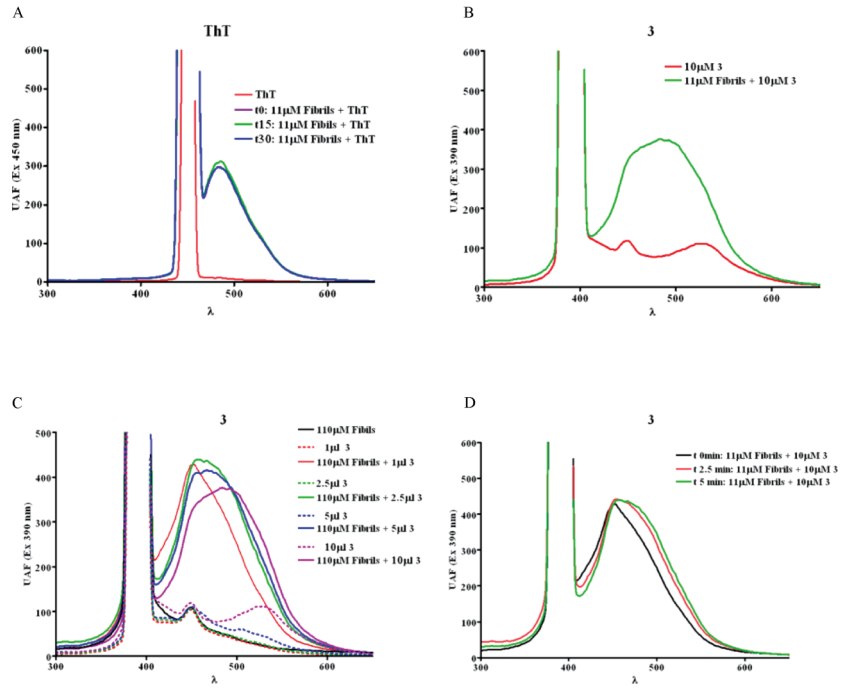

Fig. 5 Fluorescent spectroscopy of ThT and **3** in the presence or the absence of β-amyloid fibrils A) ThT at various temperature, B) **3** at 10 μM with and without fibrils; C) **3** and fibrils at various concentrations; and D) **3** at different incubation times.

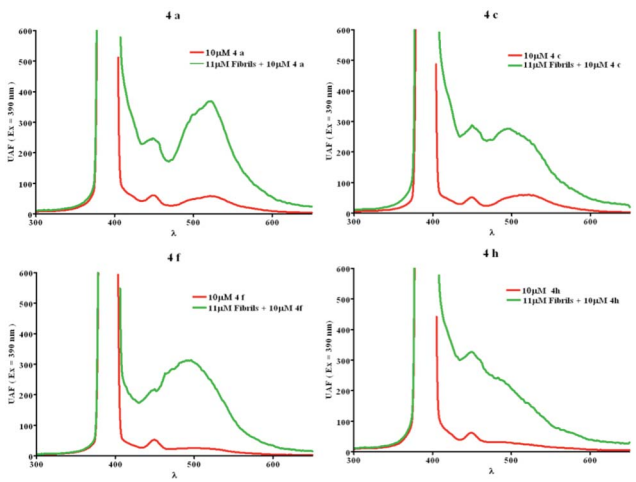

Fig. 6 Fluorescence spectroscopy of compounds **4a**,**c**,**f**,**h** (10μM) in the absence (red) or in the presence of $A\beta_{1\text{-}42}$ fibrils (green). The addition of fibrils changed significantly the emission spectra of the compounds.

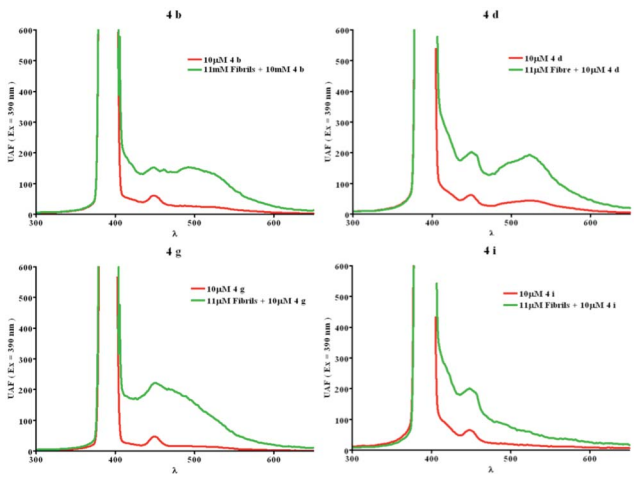

Fig. 7 Fluorescence spectroscopy of compounds **4b**,**d**,**g**,**i** (10 μM) in the absence (red) or in the presence of $A\beta_{1\text{-}42}$ fibrils (green). The addition of fibrils slightly altered the emission spectra of the compounds.

plaques in brain tissue preparations was identified. The analyzed compounds showed a fluorescence behaviour similar to that of classic amyloid fluorescence probes such as ThT and Congo Red. It is also worth noticing that selected compounds **4a–c** do not alter the Aβ fibrils stability as assessed by EM analysis and by quantitative measurement of aggregated $A\beta_{1\text{-}42}$ after treatment with these staining agents. These compounds represent a novel chemotype to be used as fluorescent probes for *in vitro* study of amyloid structures. Moreover, due to their ability to cross the BBB and concentrate in the mouse brain, a prospective application of these compounds could be as potential amyloid imaging agents.

Experimental section

General information

Reagents were purchased from Aldrich and were used as received. Reaction progress was monitored by TLC using Merck silica gel 60 F_{254} (0.040–0.063 mm) with detection by UV. Merck silica gel 60 (0.040–0.063 mm) was used for column chromatography. Melting points were determined in Pyrex capillary tubes using an Electrothermal 8103 apparatus and are uncorrected. ^{1}H NMR and ^{13}C NMR spectra were recorded on Brüker 200 MHz or Varian 300 MHz or Varian 500 MHz spectrometers by using the residual signal of the deuterated solvent as internal standard. Splitting

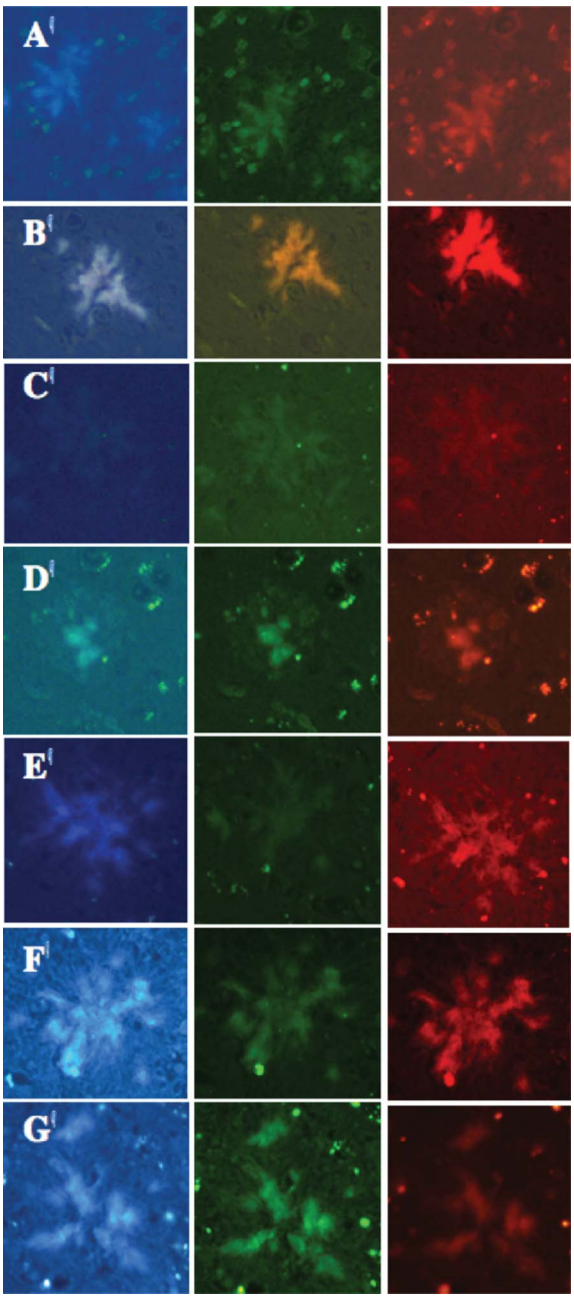

Fig. 8 Amyloid plaques in parenkyma sections from temporal cortex of Tg CRND8 mice incubated with compounds **ThS** (A), **2** (B), **3** (C), **4a** (D), **4b** (E), **4f** (F), **4g** (G) at 0.5 mM. Fluorescent sections were viewed using fluoromicroscope UV, FITC, and TRITC.

patterns are described as singlet (s), doublet (d), triplet (t), quartet (q), and broad (br); the value of chemical shifts (δ) are given in ppm and coupling constants (J) in Hertz (Hz). ESI-MS spectra were performed by an Agilent 1100 Series LC/MSD spectrometer. HPLC analysis were performed by a LaPrep P130 apparatus using a P311 UV detector. Yields refer to purified products and are not optimised. All moisture-sensitive reactions were performed under argon atmosphere using oven-dried glassware and anhydrous solvents. All the organic layers were dried using anhydrous sodium sulfate. Purity of tested compounds is ≥95% as determined by elemental analysis. Elemental analyses were performed in a Perkin-

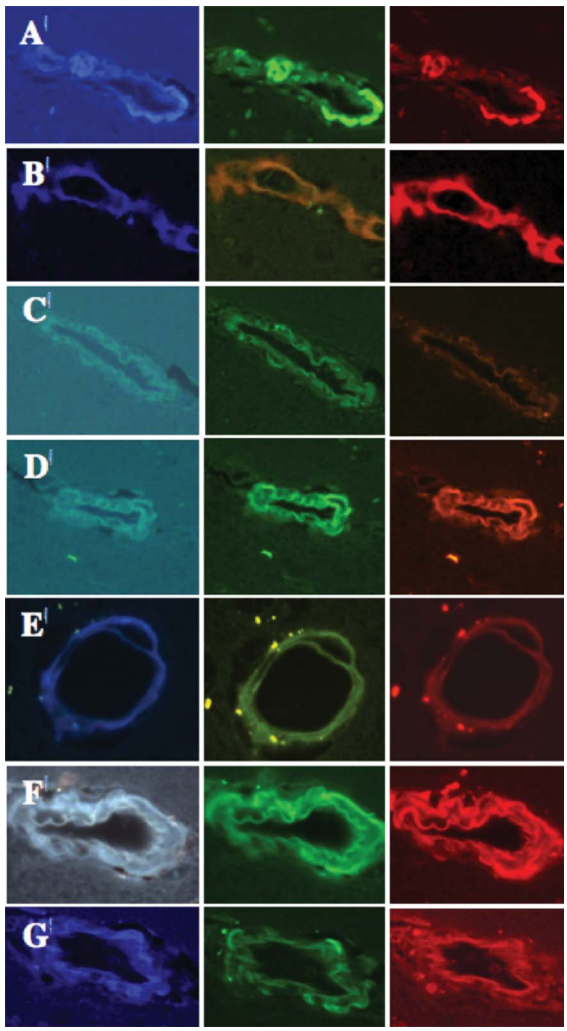

Fig. 9 Amyloid deposits in vascular walls sections from temporal cortex of Tg CRND8 mice incubated with compounds **ThS** (A), **2** (B), **3** (C), **4a** (D), **4b** (E), **4f** (F), **4g** (G) at 0.5 mM. Fluorescent sections were viewed using fluoromicroscope UV, FITC, and TRITC.

Elmer 240C elemental analyser and the results were within ± 0.4% of the theoretical values, unless otherwise noted. Intermediates **7a–c**,**f–h** were prepared as previously described.[20,28,29] Compound **3** was prepared as previously described[15] and here has been reported its full characterization.

3-Nitro-4-(1*H*-pyrrol-1-yl)benzoic acid (9). 2,5-Dimethoxytetrahydrofuran (3.5 mL, 27.7 mmol) was added to a solution of 4-amino-3-nitrobenzoic acid **8** (5.0 g, 27.4 mmol) in glacial acetic acid (25 mL) heated to 120 °C. After 1 h, the reaction mixture was cooled to 25 °C, the volatiles were evaporated and the residue was purified by column chromathography (1 : 20 MeOH/$CHCl_3$) to afford acid **9** as a yellow low melting solid (6.0 g, 94%): IR ν_{max} ($CHCl_3$; cm^{-1}) 1690; δ_H (300 MHz, DMSO-d_6) 13.69 (s, 1H), 8.43 (d, J = 1.8 Hz, 1H), 8.24 (dd, J = 8.4, 1.9 Hz, 1H), 7.75 (d, J = 8.4 Hz, 1H), 7.13–6.87 (m, 2H) and 6.43–6.19 (m, 2H); δ_C (100 MHz, DMSO-d_6) 165.7, 144.5, 136.9, 134.8, 130.5, 128.5, 126.6, 122.0 and 112.1; m/z (ESI) 231 $(M\text{-}H)^-$; m/z HRMS (ESI) $[M - H]^-$ calcd 231.0406 for $C_{11}H_7N_2O_4$, found 231.0411; Elemental calcd. C, 56.90; H, 3.47; N, 12.06 for $C_{11}H_8N_2O_4$; found C, 57.10; H, 3.78; N, 12.12.

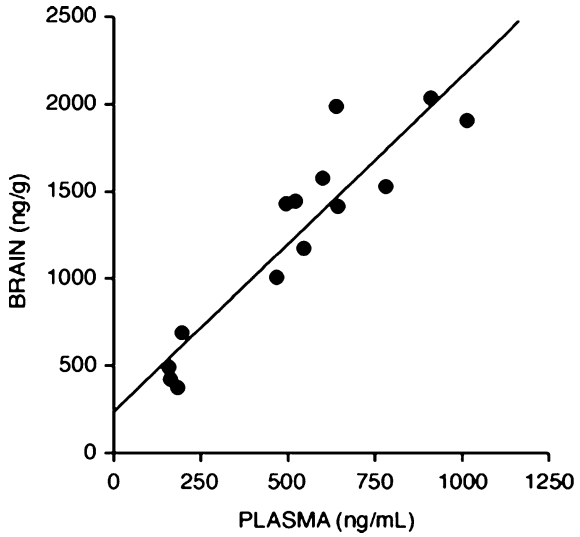

Fig. 10 Relationship between whole brain and plasma concentrations of compound **4c** after intraperitoneal doses of 1.25–10 mg/kg.

3-Amino-4-(1*H*-pyrrol-1-yl)benzoic acid (10). A mixture of **9** (2.0 g, 8.6 mmol) and a catalytic amount of 10% palladium on carbon in a 1 : 1 EtOAc/MeOH (20 mL) was stirred at 25 °C under an H_2 atmosphere for 14 h. The reaction mixture was filtered through Celite and the filtrate was concentrated. The pale yellow low melting solid thus obtained (**10**, 1.6 g, 92%) was used in the next step without further purification: IR ν_{max} ($CHCl_3$; cm^{-1}) 3609, 3330 and 1685; δ_H (300 MHz, DMSO-d_6) 12.75 (bs, 1H), 7.47 (d, J = 1.8 Hz, 1H), 7.19 (dd, J = 8.1, 1.8 Hz, 1H), 7.10 (d, J = 8.1 Hz, 1H), 6.95 (t, J = 2.1 Hz, 2H), 6.25 (t, J = 2.1 Hz, 2H) and 5.10 (bs, 2H); m/z (ESI) $(M-H)^-$ 201; m/z HRMS (ESI) $[M+H]^+$ calcd 203.0821 for $C_{11}H_{11}N_2O_2$, found 203.0827; Elemental calcd. C, 65.34; H, 4.98; N, 13.85 for $C_{11}H_{10}N_2O_2$; found C, 65.48; H, 4.71; N, 14.04.

7-Carboxypyrrolo[1,2-*a*]quinoxalin-4(5*H*)one (6). A mixture of aniline **10** (1.0 g, 4.34 mmol) and triphosgene (0.42 g, 1.43 mmol) in dry toluene (20 mL) was stirred under reflux. After 4 h the reaction mixture was cooled to 25 °C and bubbled with a stream of nitrogen overnight. The resulting solid was washed with EtOAc to afford **6** (0.74 g, 75%) as white prisms after recrystallization (hexane): mp > 300 °C (hexane); IR ν_{max} ($CHCl_3$; cm^{-1}) 1782 and 1715; δ_H (300 MHz, DMSO-d_6) 13.04 (s, 1H), 11.42 (s, 1H), 8.23 (d, J = 1.3 Hz, 1H), 8.13 (d, J = 8.6 Hz, 1H), 7.89 (d, J = 1.6 Hz, 1H), 7.73 (dd, J = 8.5, 1.6 Hz, 1H), 7.06 (dd, J = 3.8, 1.0 Hz, 1H) and 6.88–6.60 (m, 1H); m/z (ESI) 227 $(M-H)^-$; m/z HRMS (ESI) $[M+H]^+$ calcd 229.0613 for $C_{12}H_9N_2O_3$, found 229.0612; Elemental calcd. C, 63.16; H, 3.53; N, 12.28 for $C_{12}H_8N_2O_3$; found C, 63.40; H, 3.65; N, 11.96.

4-Hydrazino-7,8-dimethylpyrrolo[1,2-*a*]quinoxaline (7d). $POCl_3$ (3.6 mL, 23.7 mmol) and *N*,*N*-dimethylaniline (0.35 mL, 2.70 mmol) were added to **5d** (0.20 g, 1.08 mmol) and the resulting mixture was heated to 120 °C for 4 h. Thereafter, the reaction mixture was cooled to room temperature, poured into ice-water (10 mL), and extracted with ethyl acetate (3 × 20 mL). The combined organic layers were washed with brine, dried over Na_2SO_4 and evaporated. The residue was purified by flash-chromatography (10% ethyl acetate in hexane) and the resulting chloride was dissolved in ethanol (10 mL). Hydrazine monohydrate (0.11 mL, 2.3 mmol) was added to the resulting mixture, and after heating under reflux for 2 h, the reaction mixture was cooled to room temperature. The precipitated solid was collected by filtration and washed with diethyl ether to afford **5d** as a white solid (171 mg, 73%): mp 280 °C (hexane); IR ν_{max} ($CHCl_3$; cm^{-1}) 3615 and 1533; δ_H (200 MHz, DMSO-d_6) 7.75–7.74 (m, 1H), 7.49–7.46 (m, 2H), 6.68–6.61 (m, 2H), 6.23 (bs, 1H), 4.22 (s, 2H), 2.38 (s, 3H) and 2.34 (s, 3H); m/z (ESI) 227$(M+H)^+$; m/z HRMS (ESI) $[M+H]^+$ calcd 227.1297 for $C_{13}H_{15}N_4$, found 227.1299; Elemental calcd. C, 69.00; H, 6.24; N, 24.76 for $C_{13}H_{14}N_4$; found C, 68.84; H, 6.62; N, 24.66.

4-Hydrazino-7-carbomethoxypyrrolo[1,2-*a*]quinoxaline (7e). A mixture of **6** (0.5 g, 2.19 mmol), $POCl_3$ (4.5 mL) and *N*,*N*-dimethylaniline (0.83 mL, 6.6 mmol) was heated to 115 °C for 3 h, afterward the reaction mixture was cooled to 0 °C. The reaction mixture was stirred in the presence of MeOH and then it was poured into water. The aqueous phase was extracted with EtOAc, the organic extracts were washed with a saturated solution of $NaHCO_3$ and dried over Na_2SO_4. The solvent was removed and the crude product was purified by column chromathography to afford the intermediate chloride (0.24 g, 45%) as a white low melting solid: δ_H (300 MHz, $CDCl_3$) 8.57 (d, J = 1.8 Hz, 1H), 8.19 (dd, J = 8.6, 1.9 Hz, 1H), 7.99 (dd, J = 2.8, 1.3 Hz, 1H), 7.85 (d, J = 8.6 Hz, 1H), 7.09 (dd, J = 4.1, 1.3 Hz, 1H), 6.94 (dd, J = 4.0, 2.8 Hz, 1H) and 3.97 (s, 3H). The above chloride was treated with hydrazine monohydrate (0.19 mL, 3.9 mmol) in refluxing methanol. After 2 h the reaction mixture was cooled to 25 °C, the solvent was removed and the resulting solid was recrystallized from MeOH to obtain **7e** as a pale yellow solid (60%): mp 185 °C (methanol); IR ν_{max} ($CHCl_3$; cm^{-1}) 3682 and 1718; δ_H (300 MHz, DMSO-d_6) 8.93 (bs, 1H), 8.26 (s, 1H), 8.14 (d, J = 8.5 Hz, 1H), 8.06 (d, J = 1.7 Hz, 1H), 7.73 (dd, J = 8.4, 1.7 Hz, 1H), 7.06 (d, J = 3.2 Hz, 1H), 6.84–6.66 (m, 1H), 4.60 (br, 2H) and 3.86 (s, 3H). m/z (ESI) 279 $(M+Na)^+$; m/z HRMS (ESI) $[M+Na]^+$ calcd 279.0858 for $C_{13}H_{12}N_4O_2Na$, found 279.0863; Elemental calcd. C, 60.93; H, 4.72; N, 21.86 for $C_{13}H_{12}N_4O_2$; found C, 61.21; H, 4.54; N, 21.61.

2-[(Quinolin-4-yl)methylene]-1-(7-methoxy-4-methylquinolin-2-yl)hydrazine (3). An equimolar mixture of 7-methoxy-4-methyl-2-hydrazinoquinoline[30] and quinoline-4-carbaldehyde was dissolved in ethanol and heated under reflux for 3 h. The title compound was isolated in 86% yield by crystallization from ethanol: mp 265 °C (ethanol); IR ν_{max} ($CHCl_3$; cm^{-1}) 1605 and 1518; δ_H (300 MHz, DMSO-d_6) 11.57 (s, 1H), 8.92 (d, J = 4.6 Hz, 1H), 8.79 (s, 1H), 8.54 (dd, J = 8.4, 1.1 Hz, 1H), 8.07 (dd, J = 8.3, 1.1 Hz, 1H), 7.93 (d, J = 4.6 Hz, 1H), 7.87–7.66 (m, 3H), 7.41 (d, J = 0.9 Hz, 1H), 7.05 (d, J = 2.5 Hz, 1H), 6.99 (dd, J = 9.0, 2.6 Hz, 1H) and 3.87 (s, 3H). m/z (ESI) 343 $(M+H)^+$; m/z HRMS (ESI) $[M+H]^+$ calcd 343.1559 for $C_{21}H_{19}N_4O$, found 343.1562; Elemental calcd. 73.67; H, 5.30; N, 16.36 for $C_{21}H_{18}N_4O$; found C, 73.53; H, 5.26; N, 16.00.

2-[(Quinolin-4-yl)methylene]-1-(7-methoxypyrrolo[1,2-*a*]quinoxalin-4-yl)hydrazine (4a). Quinoline-4-carbaldehyde (40 mg, 0.25 mmol) was added to a solution of **7a** (46 mg, 0.23 mmol) in ethanol (6 mL) and the resulting mixture was heated under reflux. After 4 h it was cooled to room temperature and the volatiles were

evaporated. The residue was chromatographed (2% methanol in chloroform) to afford **4a** as a yellow solid (72.8 mg, 94%): mp 201 °C (ethanol). R_t 8.6, 10.6 min [MeCN]. IR ν_{max} ($CHCl_3$; cm^{-1}) 3680, 3372, 1622, 1610 and 1541; δ_H (500 MHz, DMSO-d_6) Tautomer A 10.70 (bs, 1H, NH-1), 9.32 (s, 1H, H-17), 9.02 (d, 1H, J = 8.2 Hz, H-26), 8.65 (d, 1H, J = 8.5 Hz, H-20), 8.50 (d, 1H, J = 8.2 Hz, H-27), 8.09 (d, 1H, J = 8.2 Hz, H-23), 7.97 (d, 1H, J = 7.5 Hz, H-9), 7.83 (dd, 1H, J = 8.2, 7.5 Hz, H-21), 7.71 (dd, 1H, J = 8.2, 7.5 Hz, H-22), 7.42 (s, 1H, H-12), 6.80 (d, 1H, J = 7.5 Hz, H-10), 7.07 (bs, 1H, H-6), 6.70 (bs, 2H, H-4, H-5) and 3.87 (s, 3H, 11-OMe); Tautomer B 11.80 (bs, 1H, NH-15), 9.32 (s, 1H, H-17), 9.02 (d, 1H, J = 8.2 Hz, H-26), 8.65 (d, 1H, J = 8.5 Hz, H-20), 8.50 (d, 1H, J = 8.2 Hz, H-27), 8.13 (d, 1H, J = 7.5 Hz, H-9), 8.09 (d, 1H, J = 8.2 Hz, H-23), 7.83 (dd, 1H, J = 8.2, 7.5 Hz, H-21), 7.71 (dd, 1H, J = 8.2, 7.5 Hz, H-22), 7.40 (s, 1H, H-12), 7.06 (d, 1H, J = 7.5 Hz, H-10), 7.05 (bs, 1H, H-6), 6.70 (bs, 2H, H-4, H-5) and 3.86 (s, 3H, 11-OMe). δ_H (300 MHz, $CDCl_3$) 9.29 (s, 1H), 9.21 (s, 1H), 8.97 (d, J = 4.4 Hz, 1H), 8.48 (d, J = 8.3 Hz, 1H), 8.16 (d, J = 8.4 Hz, 1H), 7.95 (d, J = 4.2 Hz, 1H), 7.80–7.69 (m, 2H), 7.64–7.59 (m, 2H), 7.53 (d, J = 9.0 Hz, 1H), 6.80–6.64 (m, 3H) and 3.86 (s, 3H); m/z (ESI) 368 $(M+H)^+$; m/z HRMS (ESI) $[M+H]^+$ calcd 368.1511 for $C_{22}H_{18}N_5O$, found 368.1515; Elemental calcd. C, 71.92; H, 4.66; N, 19.06 for $C_{22}H_{17}N_5O$; found C, 71.64; H, 4.49; N, 19.31.

2-[(Quinolin-4-yl)methylene]-1-(pyrrolo[1,2-*a*]quinoxalin-4-yl) hydrazine (4b). Starting from **7b**, the title compound was prepared as above described and it was obtained in 89% yield as a yellow solid: mp 226 °C (ethanol). R_t 9.1, 11.4 min [MeCN]. IR ν_{max} ($CHCl_3$; cm^{-1}) 3376, 1652, 1611, 1537 and 1433; δ_H (300 MHz, $CDCl_3$) 9.34 (s, 1H), 9.28 (s, 1H), 9.00 (d, J = 4.6 Hz, 1H), 8.54 (d, J = 8.5 Hz, 1H), 8.18 (d, J = 8.5 Hz, 1H), 7.98 (d, J = 4.6 Hz, 1H), 7.82–7.73 (m, 1H), 7.73–7.69 (m, 1H), 7.69–7.61 (m, 2H), 7.31–7.14 (m, 4H) and 6.75–6.70 (m, 1H); m/z (ESI) 338 $(M+H)^+$; m/z HRMS (ESI) $[M+H]^+$ calcd 338.1406 for $C_{21}H_{16}N_5$, found 338.1400; Elemental calcd. C, 74.76; H, 4.48; N, 20.76 for $C_{21}H_{15}N_5$; found C, 74.38; H, 4.70; N, 20.52.

2-[(Quinolin-4-yl)methylene]-1-(7-fluoropyrrolo[1,2-*a*]quinoxalin-4-yl)hydrazine (4c). Starting from **7c** (60 mg, 0.28 mmol), the title compound was prepared following the above described procedure and was obtained as a yellow solid (72 mg, 73%): mp 233 °C (ethanol). R_t 8.4, 10.6 [MeCN]. IR ν_{max} ($CHCl_3$; cm^{-1}) 3508 and 1609; δ_H (300 MHz, $CDCl_3$) 9.37 (s, 1H), 9.27 (s, 1H), 8.99 (d, J = 4.6 Hz, 1H), 8.49 (d, J = 8.4 Hz, 1H), 8.18 (d, J = 8.5 Hz, 1H), 7.95 (d, J = 4.4 Hz, 1H), 7.77 (ddd, J = 8.4, 6.9, 1.4 Hz, 1H), 7.69–7.55 (m, 3H), 7.01–6.84 (m, 3H) and 6.76–6.69 (m, 1H); m/z (ESI) 356 $(M+H)^+$; m/z HRMS (ESI) $[M+H]^+$ calcd 356.1311 for $C_{21}H_{15}FN_5$, found 356.1314; Elemental calcd. C, 70.98; H, 3.97; N, 19.71 for $C_{21}H_{14}FN_5$; found C, 71.19; H, 4.26; N, 19.45.

2-[(Quinolin-4-yl)methylene]-1-(7,8-dimethylpyrrolo[1,2-*a*]quinoxalin-4-yl)hydrazine (4d). Starting from **7d** (250 mg, 1.44 mmol), the title compound was prepared following the above described procedure and was obtained as a yellow solid (182 mg, 45%): mp 265 °C (ethanol). R_t 8.4, 10.6 [MeOH]. IR ν_{max} ($CHCl_3$; cm^{-1}) 3688 and 1603; δ_H (200 MHz, $CDCl_3$) 9.24 (br, 2H), 8.95 (d, 1H, J = 5.0 Hz), 8.47 (d, 1H, J = 8.4 Hz), 8.15 (d, 1H, J = 8.2 Hz), 7.98 (d, 1H, J = 4.5 Hz), 7.79–7.58 (m, 4H), 7.39 (s, 1H), 7.12 (s, 1H), 6.72 (s, 1H), 2.35 (s, 3H) and 2.32 (s, 3H); m/z (ESI) 366 $(M+H)^+$; m/z HRMS (ESI) $[M+H]^+$ calcd 366.1719 for $C_{23}H_{20}N_5$, found 366.1725; Elemental calcd. C, 75.59; H, 5.24; N, 19.16 for $C_{23}H_{19}N_5$; found C, 75.70; H, 4.92; N, 19.28.

2-[(Quinolin-4-yl)methylene]-1-(7-carbomethoxypyrrolo[1,2-*a*]quinoxalin-4-yl)hydrazine (4e). Starting from **7e** the title compound was prepared following the above described procedure and was obtained as a yellow solid: mp 227 °C (ethanol). IR ν_{max} ($CHCl_3$; cm^{-1}) 1722, 1625, 1551, 1524 and 1433; δ_H (200 MHz, $CDCl_3$) 9.44 (s, 1H), 9.18 (s, 1H), 8.92 (d, J = 4.5 Hz, 1H), 8.39 (d, J = 8.4 Hz, 1H), 8.12 (dd, J = 8.5, 0.8 Hz, 1H), 7.90 (d, J = 4.5 Hz, 1H), 7.85 (s, 1H), 7.81–7.66 (m, 2H), 7.56 (dd, J = 18.8, 8.6 Hz, 3H), 7.24 (d, J = 3.4 Hz, 1H), 6.78–6.65 (m, 1H) and 3.92 (s, 3H); m/z (ESI) 396 $(M+H)^+$; m/z HRMS (ESI) $[M+H]^+$ calcd 396.1460 for $C_{23}H_{18}N_5O_2$, found 396.1455; Elemental calcd. C, 69.86; H, 4.33; N, 17.71 for $C_{23}H_{17}N_5O_2$; found C, 70.13; H, 4.37; N, 17.41.

2-[(Quinolin-4-yl)methylene]-1-(pyrido[3,2-*e*]pyrrolo[1,2-*a*]pyrazin-6-yl)hydrazine (4f). Starting from **7f** (54 mg, 0.27 mmol), the title compound was prepared following the above described procedure and was obtained as a yellow solid (60 mg, 65%): mp 236 °C (ethanol). R_t 9.4, 12.0 [MeCN]. IR ν_{max} ($CHCl_3$; cm^{-1}) 3623, 1620 and 1532; δ_H (300 MHz, $CDCl_3$) 9.29 (s, 1H), 9.12 (s, 1H), 9.00 (d, J = 4.5 Hz, 1H), 8.49 (d, J = 8.2 Hz, 1H), 8.28–8.07 (m, 2H), 7.95 (d, J = 3.4 Hz, 1H), 7.82–7.73 (m, 1H), 7.70–7.58 (m, 1H), 7.58–7.43 (m, 1H), 7.38–7.21 (m, 3H) and 6.86–6.67 (m, 1H); m/z (ESI) 339 $(M+H)^+$; m/z HRMS (ESI) $[M+H]^+$ calcd 339.1358 for $C_{20}H_{15}N_6$, found 339.1360; Elemental calcd. C, 70.99; H, 4.17; N, 24.84 for $C_{20}H_{14}N_6$; found C, 71.25; H, 3.98; N, 24.63.

2-[(Quinolin-4-yl)methylene]-1-(imidazo[1,2-*a*]quinoxalin-4-yl)-hydrazine (4g). To a solution of **7a** (46 mg, 0.23 mmol) in ethanol (6 mL) was added quinoline-4-carbaldehyde (40 mg, 0.25 mmol) to room temperature and then resulting mixture was refluxed for 4h at 90 °C. Thereafter, the reaction mixture was cooled to room temperature and evaporated. The residue was chromatographed (2% methanol in chloroform) to afford **7a** as a dark yellow solid (40 mg, 51%): mp 258 °C (ethanol). IR ν_{max} ($CHCl_3$; cm^{-1}) 1596; δ_H (300 MHz, $CDCl_3$) 10.08 (s, 1H), 9.49 (s, 1H), 9.00 (d, J = 4.8 Hz, 1H), 8.46 (d, J = 8.5 Hz, 1H), 8.18 (d, J = 8.3 Hz, 1H), 8.12–7.96 (m, 2H), 7.83–7.73 (m, 1H), 7.73–7.60 (m, 2H), 7.60–7.43 (m, 1H) and 7.41–7.20 (m, 3H). m/z (ESI) 339 $(M+H)^+$; m/z HRMS (ESI) $[M+H]^+$ calcd 339.1358 for $C_{20}H_{15}N_6$, found 339.1351; Elemental calcd. C, 70.99; H, 4.17; N, 24.84 for $C_{20}H_{14}N_6$; found C, 70.94; H, 3.83; N, 24.47.

2-[(Quinolin-4-yl)methylene]-1-(7-fluoroimidazo[1,2-a]quinoxalin-4-yl)hydrazine (4h). Starting from **7b** (0.16 g, 0.73 mmol), the title compound was prepared following the above described procedure and was obtained as a yellow solid (0.24 g, 90%): mp 286 °C (ethanol). R_t 7.2, 9.3 [MeCN]. IR ν_{max} 1545 and 1510 ($CHCl_3$; cm^{-1}) 1545 and 1510; δ_H (300 MHz, $CDCl_3$) 9.92 (s, 1H), 9.51 (s, 1H), 9.01 (d, J = 4.6 Hz, 1H), 8.95 (s, 1H), 8.61 (d, J = 8.3 Hz, 1H), 8.20 (d, J = 8.1 Hz, 1H), 8.08–7.98 (m, 2H), 7.84–7.64 (m, 3H), 7.23–7.16 (m, 1H) and 7.08–6.89 (m, 1H). m/z (ESI) 357 $(M+H)^+$; m/z HRMS (ESI) $[M+H]^+$ calcd 357.1264 for $C_{20}H_{14}FN_6$, found 357.1260; Elemental calcd. C, 67.41; H, 3.68; N, 23.58 for $C_{20}H_{13}FN_6$; found C, 67.56; H, 3.55; N, 23.81.

2-[(Quinolin-2-yl)methylene]-1-(pyrrolo[1,2-*a*]quinoxalin-4-yl)-hydrazine (4i). Starting from **7a** and quinoline-2-carboxyaldehyde and following the above described procedure, the title compound was obtained in 85% yield as a yellow solid: mp 189 °C (ethanol). IR ν_{max} ($CHCl_3$; cm^{-1}) 3676, 1628, 1536 and 1430; δ_H (200 MHz, $CDCl_3$) 9.50 (s, 1H), 8.77 (s, 1H), 8.22–8.06 (m, 3H), 7.78 (d, J = 8.0 Hz, 1H), 7.74–7.65 (m, 1H), 7.62 (s, 1H), 7.58–7.45 (m, 2H), 7.29–7.22 (m, 1H), 7.20 (d, J = 4.0 Hz, 2H), 7.15–7.04 (m, 1H) and 6.75–6.58 (m, 1H). m/z (ESI) 338 $(M+H)^+$; m/z HRMS (ESI) $[M+H]^+$ calcd 338.1406 for $C_{21}H_{16}N_5$, found 338.1411; Elemental calcd. C, 74.76; H, 4.48; N, 20.76 for $C_{21}H_{15}N_5$; found C, 74.42; H, 4.40; N, 20.66.

X-Ray crystallography of 4a

Single crystals of **4a** were obtained by dissolving some mg in ethanol or methanol and allowing the solution to concentrate at room temperature. Two sets of polymorphic crystals were obtained: from ethanol, lath orange crystals (**4a**$_a$) of approximate dimensions 0.2 × 0.09 × 0.02 mm were produced, while from methanol slab pale orange crystals (**4a**$_b$) of approximate dimensions 0.1 × 0.1 × 0.03 mm were obtained. A crystal of each set was submitted to X-ray diffraction by using a Bruker-Nonius FR591 rotating anode diffractometer with graphite monochromated Mo-Kα radiation (λ = 0.71073 Å). The structures were solved by direct methods implemented in the SHELXS-97 program.[31] The refinements were carried out by full-matrix anisotropic least-squares on F^2 for all reflections for non-H atoms by using the SHELXL-97 program.[32] Absorption correction obtained by SADABS[33] was applied to both the data collections.

4a$_a$: $C_{22}H_{17}N_5O \times H_2O$ (mol wt 385.4). Crystal system: orthorhombic, space group $P2_12_12_1$ (n 19); a = 4.8025(2), b = 11.5872(8), c = 33.050(2) Å, V = 1839.17(19) $Å^3$, Z = 4, Dc = 1.392 g cm^{-13}. 28594 reflections were collected at −153 °C of which 4048 are unique (R_{int} = 0.10). Final refinement converged to R_1 = 0.057, wR_2 = 0.097 for I>2σI, goodness-of-fit = 1.03. Min. max height in last Δρ map of −0.21 and 0.20 e$Å^{-3}$.

4a$_b$: $C_{22}H_{17}N_5O \times 0.58\ H_2O \times 0.42\ CH_3OH$ (mol wt 391.1). Crystal system: monoclinic, space group $C2/c$ (n. 15); a = 24.252(3), b = 9.3398(11), c = 17.6282(17) Å, β = 102.784(5)°, V = 3894.0(8) $Å^3$, Z = 8, Dc = 1.324 g cm^{-13}. 19860 reflections were collected at −153 °C of which 3420 are unique (R_{int} = 0.09). Final refinement converged to R_1 = 0.093, wR_2 = 0.218 for $I>2\sigma I$, goodness-of-fit = 1.09. Min max height in last Δρ map of −0.30 and 0.39 e$Å^{-3}$. The compound crystallized with a water molecule having site occupation factor (s.o.f.) equal to 0.58(1) and with a disordered methanol molecule (s.o.f. 0.42(1)).

Interference with ThT Binding

Synthetic $A\beta_{1-42}$ (Tecnogen, Caserta, Italy) was dissolved at a concentration of 0.11 mM in H_2O/MeCN (1 : 1 = v : v), and aliquots of the solution containing 15 μg were lyophilized. Samples were dissolved in 15 μl of 10 mM NaOH, mixed with 15 μl of 100 mM Tris-HCl buffer, pH 7.4 and incubated for 5 days at 37 °C. Samples were then centrifuged at 13,000 rpm for 10 min, the supernatants were discharged and the pellets resuspended in 30 μL of the same buffer containing the test compounds at the concentration of 110 μM. After 30 min of incubation the samples were centrifuged for 10 min at 13,000 rpm, the pellets were resuspended in 300 μL of 50 mM glycine–NaOH buffer, pH 9.6 containing a solution of 2 μM ThT. The samples were incubated for 5 min and the fluorescence was determined by spectrophotofluorimetry (LS 5OB Perkin Elmer Instr., Bekomfield, UK) at the excitation and emission wave lengths of 420 and 480 nm, respectively. The ability of test compounds to interfere with ThT fluorescence increase was evaluated using preformed $A\beta_{1-42}$ fibers as positive controls.

HPLC determination of $A\beta_{1-42}$

A solution of synthetic peptide $A\beta_{1-42}$ in Tris-HCl 100 mM, pH 7.4 (Merck, Darmstadt, Germany) was incubated for 5 d at 37 °C in the presence of the examined compounds. After centrifugation at 13,000 X rpm for 10 min at 4 °C, the pellets were dissolved in 80 μL of 10% formic acid containing 0.1% trifluoroacetic acid and analyzed by RP-HPLC.[34] Parallel samples were run in the absence of compounds. The results were calculated as percentage of peptide present in this condition.

Electron microscopy

The synthetic peptide $A\beta_{1-42}$ was suspended in 100 mM Tris-HCl, pH 7.4, at a concentration of 0.11 mM either in the presence or in the absence of equimolar concentration of the compounds. Following 5 d incubation at 37 °C, 5 μL aliquots of peptide suspension were applied to Formvar-coated nickel grids, negatively stained with 5% (w/v) uranyl acetate, and observed in an electron microscope (EM 109, Zeiss, Germany) at 80 kV.

Sections staining

Brains from Tg CRND8 mice encoding a double mutant form of amyloid precursor protein 695 (KM670/671NL+V717F) under the control of the PrP gene promoter[26] were dissected. Parts of the brain were fixed in Carnoy and embedded in paraffin. Five-micrometre-thick serial sections of paraffin-embedded blocks from the temporal cortex were used for staining. Paraffin sections were first taken through five 10 min incubations in xylene, five 10 min incubations in 100% EtOH to completely deparaffinize. Tissue sections were covered with a solution of EtOH 96% with the different compounds at 0.5 mM. After 30 min of incubation the sections were washed in EtOH 96% Thereafter, the sections were incubated in EtOH 100% and xylene before to apply the coverslip. Fluorescent sections were viewed using fluoromicroscope (Olympus BX 61) with M-3204C CCD equipped with filters UV (Ex 330–385 nm/Em > 420), FITC (Ex 450–480 nm/Em > 515) and TRITC (Ex 530–550 nm/Em >590). Because *in vitro* studies using compound bound to synthetic amyloid demonstrated that maximal emission of compound excited at 370 nm occurred at 481 nm, the filters cube were appropriate for examination of compounds. The staining of compounds were compared to Thioflavin S and Congo red staining.[35]

Fluorescence spectroscopy

To investigate the binding of the compounds to A_{1-42}, aliquots of 15 μg of peptide were dissolved in 15 μl of NaOH 10 mM, added with 15 μl of Tris-HCl buffer 100 mM (pH 7.4) and the samples were incubated at 37 °C for one week. After this time the samples

were centrifuged at 13,000 rpm for ten minutes the supernatant was discharged and the pellet of fibrils was resuspended in 300 µl of 50 mM glycine-NaOH buffer, pH 9.6 including test compounds, 10 µM. Five minutes after dilution the emission spectra were determined with a Perkin Elmer LS 50B spectrophotofluorimeter in the range of 300–650 nm with excitation wavelengths of 390 nm. In parallel the alone test compounds and the alone fibrils were analyzed at the same concentration and conditions. To calculate the binding to $A\beta_{1\text{-}42}$ the fluorescence of solutions of the test drugs alone was subtracted from that of samples containing the fibrils and the drug.

Drug Administration and Plasma and Brain Sampling

Male CD1 mice weighing about 25 g (Charles River, Italy) were used. Procedures involving animals and their care were conducted in conformity with the institutional guidelines that are in compliance with national (D.L. n. 116, G.U., suppl. 40, 18 Febbraio 1992, Circolare No. 8, G.U., 14 Luglio 1994) and international laws and policies (EEC Council Directive 86/609, OJ L 358,1, Dec. 12, 1987; Guide for the Care and Use of Laboratory Animals, U.S. National Research Council, 1996). Animals (n = 15) were given the test compound intraperitoneally (1, 2.5, 5 and 10 mg kg^{-1}, dissolved in PEG-400:DMSO:ethanol (70 : 20 : 10, v/v) and were killed by decapitation under deep anaesthesia at various times after dosing. Blood samples were collected in heparinized tubes, centrifuged and the plasma was stored at –20 °C. Brains were rapidly removed, blotted with paper to remove excess surface blood and stored at –20 °C until analysis.

Drug Analysis

To 0.2 mL of plasma, a methanolic solution of the internal standard and 15 µL of 1 M sodium hydroxide were added, and the samples were extracted with 1 mL of ethyl acetate. After centrifugation, the organic phase was evaporated to dryness, the residue was dissolved in the mobile phase and analyzed by HPLC with ultraviolet detection at 254 nm. Brain tissue was homogenized in MeCN–0.01 M phosphate buffer, pH 3.5 (50 : 50 v/v; 1 g/10 mL) and a volume (2 mL) containing approximately 200 mg of tissue was extracted with 10 mL of ethyl acetate and then processed as described for plasma. Separation was done on a Discovery C18 (15 cm x 4.6 mm I.D., 5 µm particle size), with a Supelguard Discovery 5 µm precolumn, at room temperature. The mobile phase was 0.01 phosphate buffer, pH 7: acetonitrile (53 : 47, v/v), delivered isocratically at a flow rate of 1 mL min^{-1}. In these experimental conditions the analytes did not show tautomeric equilibrium and retention times were 13.8 and 6.7 min, for compound **4c** and its internal standard, respectively. Standard curves (125 to 2500 ng mL^{-1} or g^{-1}) were prepared by spiking blank mouse plasma and brain homogenate. The lower limit for quantification was about 125 ng mL^{-1} or g, using respectively 0.2 mL of plasma and 2 mL of brain homogenate (or approximately 200 mg of brain tissue). At these concentrations the coefficient of variation for the precision of the assay was 10–20%. Higher concentrations generally gave coefficients of variation less than 10%, regardless of the compound and tissue analyzed.

Acknowledgements

The Authors thank NatSynDrugs and MIUR (PRIN) for financial support.

Notes and references

1 C. Balducci, M. Beeg, M. Stravalaci, A. Bastone, A. Sclip, E. Biasini, L. Tapella, L. Colombo, C. Manzoni, T. Borsello, R. Chiesa, M. Gobbi, M. Salmona and G. Forloni, *Proc. Natl. Acad. Sci. U. S. A.*, 2010, **107**, 2295–2300.
2 R. E. Tanzi, *Nat. Neurosci.*, 2005, **8**, 977–979.
3 A. I. Bush and R. E. Tanzi, *Neurotherapeutics*, 2008, **5**, 421–432.
4 A. Lockhart, *Drug Discov. Today*, 2006, **11**, 1093–1099.
5 L. Cai, R. B. Innis and V. W. Pike, *Curr. Med. Chem.*, 2007, **14**, 19–52.
6 C. A. Mathis, Y. Wang, D. P. Holt, G. F. Huang, M. L. Debnath and W. E. Klunk, *J. Med. Chem.*, 2003, **46**, 2740–2754.
7 W. E. Klunk, H. Engler, A. Nordberg, Y. Wang, G. Blomqvist, D. P. Holt, M. Bergstrom, I. Savitcheva, G. F. Huang, S. Estrada, B. Ausen, M. L. Debnath, J. Barletta, J. C. Price, J. Sandell, B. J. Lopresti, A. Wall, P. Koivisto, G. Antoni, C. A. Mathis and B. Langstrom, *Ann. Neurol.*, 2004, **55**, 306–319.
8 M. P. Kung, C. Hou, Z. P. Zhuang, B. Zhang, D. Skovronsky, J. Q. Trojanowski, V. M. Lee and H. F. Kung, *Brain Res.*, 2002, **956**, 202–210.
9 A. B. Newberg, N. A. Wintering, K. Plossl, J. Hochold, M. G. Stabin, M. Watson, D. Skovronsky, C. M. Clark, M. P. Kung and H. F. Kung, *J. Nucl. Med.*, 2006, **47**, 748–754.
10 M. Ono, A. Wilson, J. Nobrega, D. Westaway, P. Verhoeff, Z. P. Zhuang, M. P. Kung and H. F. Kung, *Nucl. Med. Biol.*, 2003, **30**, 565–571.
11 N. P. Verhoeff, A. A. Wilson, S. Takeshita, L. Trop, D. Hussey, K. Singh, H. F. Kung, M. P. Kung and S. Houle, *Am. J. Geriatr. Psychiatry*, 2004, **12**, 584–595.
12 C. C. Rowe, U. Ackerman, W. Browne, R. Mulligan, K. L. Pike, G. O'Keefe, H. Tochon-Danguy, G. Chan, S. U. Berlangieri, G. Jones, K. L. Dickinson-Rowe, H. P. Kung, W. Zhang, M. P. Kung, D. Skovronsky, T. Dyrks, G. Holl, S. Krause, M. Friebe, L. Lehman, S. Lindemann, L. M. Dinkelborg, C. L. Masters and V. L. Villemagne, *Lancet Neurol.*, 2008, **7**, 129–135.
13 E. D. Agdeppa, V. Kepe, J. Liu, S. Flores-Torres, N. Satyamurthy, A. Petric, G. M. Cole, G. W. Small, S. C. Huang and J. R. Barrio, *J. Neurosci.*, 2001, **21**, RC189.
14 K. Shoghi-Jadid, G. W. Small, E. D. Agdeppa, V. Kepe, L. M. Ercoli, P. Siddarth, S. Read, N. Satyamurthy, A. Petric, S. C. Huang and J. R. Barrio, *Am. J. Geriatr. Psychiatry*, 2002, **10**, 24–35.
15 T. J. Raub, S. P. Tanis, A. E. Bhul, D. B. Carter, T. Bandiera, J. Lansen, C. Pellerano, L. Savini, 2002, WO0224652A1.
16 H. Naiki, K. Higuchi, M. Hosokawa and T. Takeda, *Anal. Biochem.*, 1989, **177**, 244–249.
17 H. LeVine, 3rd, *Protein Sci.*, 1993, **2**, 404–410.
18 W. Dzwolak and M. Pecul, *FEBS Lett.*, 2005, **579**, 6601–6603.
19 M. R. Krebs, E. H. Bromley and A. M. Donald, *J. Struct. Biol.*, 2005, **149**, 30–37.
20 G. Campiani, E. Morelli, S. Gemma, V. Nacci, S. Butini, M. Hamon, E. Novellino, G. Greco, A. Cagnotto, M. Goegan, L. Cervo, F. Dalla Valle, C. Fracasso, S. Caccia and T. Mennini, *J. Med. Chem.*, 1999, **42**, 4362–4379.
21 A. R. Katritzky, M. Karelson and P. A. Harris, *Heterocycles*, 1991, **32**, 329–369.
22 Y. P. Kitaev, B. I. Buzykin and T. V. Troepolskaya, *Russ. Chem. Rev.*, 1970, **39**, 441–456.
23 G. Giorgi, F. Ponticelli, L. Savini, L. Chiasserini and C. Pellerano, *J. Chem. Soc., Perkin Trans. 2*, 2000, 2259–2264.
24 J. T. Mague, S. Vang, D. G. Berge and W. F. Wacholtz, *Acta Crystallogr., Sect. C: Cryst. Struct. Commun.*, 1997, **53**, 973–979.
25 M. F. Zady and J. L. Wong, *J. Org. Chem.*, 1976, **41**, 2491–2495.
26 M. A. Chishti, D. S. Yang, C. Janus, A. L. Phinney, P. Horne, J. Pearson, R. Strome, N. Zuker, J. Loukides, J. French, S. Turner, G. Lozza, M. Grilli, S. Kunicki, C. Morissette, J. Paquette, F. Gervais, C. Bergeron, P. E. Fraser, G. A. Carlson, P. S. George-Hyslop and D. Westaway, *J. Biol. Chem.*, 2001, **276**, 21562–21570.

27 G. Campiani, A. Cappelli, V. Nacci, M. Anzini, S. Vomero, M. Hamon, A. Cagnotto, C. Fracasso, C. Uboldi, S. Caccia, S. Consolo and T. Mennini, *J. Med. Chem.*, 1997, **40**, 3670–3678.
28 G. Maga, S. Gemma, C. Fattorusso, G. A. Locatelli, S. Butini, M. Persico, G. Kukreja, M. P. Romano, L. Chiasserini, L. Savini, E. Novellino, V. Nacci, S. Spadari and G. Campiani, *Biochemistry*, 2005, **44**, 9637–9644.
29 F. Grande, F. Aiello, O. D. Grazia, A. Brizzi, A. Garofalo and N. Neamati, *Bioorg. Med. Chem.*, 2007, **15**, 288–294.
30 L. Savini, L. Chiasserini, V. Travagli, C. Pellerano, E. Novellino, S. Cosentino and M. B. Pisano, *Eur. J. Med. Chem.*, 2004, **39**, 113–122.
31 G. M. Sheldrick, *SHELXS-97*, Rel. 97-2, A program for automatic solution of crystal structures, Göttingen University, 1997.
32 G. M. Sheldrick, *SHELXL-97*, Rel. 97-2, A program for crystal structure refinement, Göttingen University, 1997.
33 G. M. Sheldrick, *SADABS. Version 2.10*, Bruker AXS Inc., Madison, Wisconsin, USA, 2003.
34 G. Forloni, L. Colombo, L. Girola, F. Tagliavini and M. Salmona, *FEBS Lett.*, 2001, **487**, 404–407.
35 G. Giaccone, F. Tagliavini, G. Linoli, C. Bouras, L. Frigerio, B. Frangione and O. Bugiani, *Neurosci. Lett.*, 1989, **97**, 232–238.

